ATCA radio imaging of the ProPlyD-like objects in the giant H II region NGC 3603

A. Mücke[1], B.S. Koribalski[2], A.F.J. Moffat[1], M.F. Corcoran[3], I.R. Stevens[4]

ABSTRACT

Three cometary-shaped objects in the giant H II region NGC 3603, originally found and identified as proto-planetary disks (ProPlyDs) by Brandner et al. (2000) using HST+VLT in the optical and near-infrared, have been detected with the Australia Telescope Compact Array (*ATCA*[1]) in the radio continuum at 3 and 6 cm. All three ProPlyD-like objects are clearly resolved with an extent of a few arcseconds. The integrated 6 cm fluxes are up to 1.3 times higher than the 3 cm fluxes with spectral indices averaged over the whole clump between $\alpha = -0.1$ and –0.5 ($S_\nu \propto \nu^\alpha$), indicating the likely presence of non-thermal emission in at least some of the sources. We present spectral index maps, and show that the sites of negative radio spectral indices are predominantly concentrated in the direction of the tails in at least two of the three ProPlyD-like nebulae while positive spectral indices are found in the region facing the ionizing star cluster. We propose that thermal bremsstrahlung and non-thermal synchrotron radiation are at work in all three ProPlyD-like sources. In at least one of the three objects optically thin non-thermal synchrotron emission appears to dominate when averaged over their whole spatial extent, while the spectrum of the second source shows a marginal indication of a non-thermal spectrum. The average spectrum of the third source is in agreement with thermal bremsstrahlung. All measured fluxes are at least one order of magnitude higher than those predicted by Brandner et al.

[1]Université de Montréal, Département de Physique, C.P. 6128, Succ. Centre-Ville, Montréal, QC, H3C 3J7, Canada, and Observatoire du Mont Mégantic; AM now at: Ruhr-Universität Bochum, Institut für Theoretische Physik, Lehrstuhl IV: Weltraum- und Astrophysik, D-44780 Bochum, Germany
email: *afm@tp4.ruhr-uni-bochum.de*, *moffat@astro.umontreal.ca*

[2]Australia Telescope National Facility, CSIRO, P.O. Box 76, Epping 1710, Australia
email: *Baerbel.Koribalski@atnf.csiro.au*

[3]Goddard Space Flight Center, NASA/GSFC Code 661, Laboratory for High Energy Astrophysics, Greenbelt, MD 20771, USA
email: *corcoran@barnegat.gsfc.nasa.gov*

[4]School of Physics & Astronomy, University of Birmingham, Birmingham B15 2TT, UK
email: *irs@star.sr.bham.ac.uk*

(2000). Upper limits for mass loss rates due to photo-evaporation are calculated to be $\sim 10^{-5}$ $M_\odot$ year^{-1} and for electron densities to be $\sim 10^4$ cm^{-3}. Due to the unexpectedly large radio luminosities of the ProPlyD-like features and because the radio emission is extended a (proto-)stellar origin of the non-thermal emission from a dust enshrouded star appears unlikely. Instead we propose that magnetized regions within the envelope of the ProPlyD-like nebulae exist.

Subject headings: interstellar medium: H II regions: individual (NGC 3603) — stars: pre-main-sequence — stars: early type, interferometry — stars: formation

1. Introduction

The giant H II region NGC 3603, located at a distance of about 6 kpc, shows the densest concentration and largest collection of visible massive stars known in our Galaxy. Recent HST images of $\sim 0''.2$ angular resolution (Moffat et al. 1994) have shown that NGC 3603 consists of three Wolf-Rayet (WR) stars and ∼70 O-type stars, with an estimated 40–50 of these stars located in the central $\sim 30'' \times 30''$ (1 pc × 1 pc) region. The three H-rich WR-stars of subtype WNL are also located within $\sim 1''$ of each other in the central core and are the brightest members of the cluster. They are believed to be massive main sequence stars which, like the bright stars in R136a, drive very strong winds (De Koter et al. 1997; Crowther and Dessart 1998). NGC 3603 has also been shown to be a seat of active star formation outside the main cluster region (e.g. Brandner et al. (2000)). In particular, three distinct dense cometary nebulae were detected there using HST and VLT: Are these ultra compact H II regions (UCHR) or ProPlyDs ?

UCHRs are small (<0.1 pc) nebulae, *internally* photoionized by a deeply embedded, massive star. Even though the embedded stars are very luminous, they are invisible at optical wavelengths because of the surrounding dust; instead they show strong far-infrared emission. Their radio continuum emission is often associated with OH and H_2O masers. The morphology of UCHRs in high resolution radio continuum images ranges from spherical, cometary, core-halo, shell, to irregular (Wood and Churchwell 1989).

In contrast, a proto-planetary disk (ProPlyD) is a phenomenon describing a low-mass, young stellar object (YSO) with a circumstellar disk, embedded in a dense (neutral and

[1]The Australia Telescope is funded by the Commonwealth of Australia for operation as a National Facility managed by CSIRO.

ionized) envelope that is being *externally* photo-evaporated by the ultraviolet radiation from one or more massive stars. These low-mass stars are not able to ionize their surroundings significantly. The disks in these systems are either observed directly (as in Orion where the disks are seen directly or in silhouette against the bright background nebula (Bally et al. 2000)), or are inferred because in almost all of the ProPlyDs (young) low-mass stars are visible at optical or near-infrared wavelengths (see e.g. Stecklum et al. (1998)). At low angular resolution ProPlyDs look like UCHRs, but at high resolution, optical and near-infrared images reveal their different nature. So most ProPlyDs would have been classified as UCHRs prior to those observations. In some cases the distinction between the two classes remains difficult. Given the fact that there are about four times more UCHRs than expected (Churchwell 1990) from star formation rates and the potential problems identifying host stars for UCHRs (e.g. some may not have enough FIR flux to account for an internal OB star), it may well be that a large fraction of catalogued UCHRs are mis-identified ProPlyDs. Interferometric radio continuum observations of ProPlyDs are needed to determine their structure, spectral indices and thus the nature of their emission, as well as mass loss rates and extinctions when compared to measured Hα fluxes.

ProPlyDs were first identified in the Orion Nebula[6], where over 150 of them are known (O'Dell et al. 1993). Two ProPlyDs have been identified in more distant nebulae: one in NGC 2024 by Stapelfeldt et al. (1997) and one, G5.97–1.17, in the Lagoon Nebula by Stecklum et al. (1998). The three ProPlyD-like objects, hereafter referred to P1, P2 and P3, in NGC 3603 (Brandner et al. 2000) are the biggest, youngest and most massive ones found *so far*. They are also the most distant known. These emission nebulae are clearly resolved in the HST/WFPC2 observations, and share the overall morphology of the ProPlyDs in Orion. All three nebulae are rim-brightened and tear-drop shaped with the tails pointing away from the central ionizing cluster.

According to Brandner et al. (2000) the brightest object (P1), which has a projected distance of 1.3 pc from the cluster, has the spectral (excitation) characteristics of a UCHR. Optical spectra reveal the presence of an underlying, heavily reddened continuum source, which is also confirmed by near-infrared VLT/ISAAC observations. The WFPC2 observations show that only the outermost layer is ionized whereas the interior is neutral. The

[6]There are a variety of different terms used in the literature for describing the knots of ionised gas in M 42 (Orion): e.g. CKs (cometary knots), PIGs (partially ionized globules), EIDERS (external ionised (accretion) disks in the environs of radiation sources), and ProPlyDs (proto-planetary disks); for a summary see McCullough et al. (1995). Another expression being used is EGGs (for evaporating gaseous globules) describing the objects found in M 16 (Eagle Nebula). The cometary knots found in the Helix Nebula are compact globules and very different from ProPlyDs as they contain no stars.

morphology of P1 is described as a heart-shaped head with a collimated structure in between, which can be understood as the superposition of two individual ProPlyDs. In contrast, P2 and P3, located at projected distances of 2.2 pc and 2.0 pc from the stellar cluster, respectively, show approximately axisymmetric morphologies. No embedded disk or central star has been detected so far in any of these nebulae, preventing a clear identification as protoplanetary disks. The optical point source (see Fig. 2c) close to P3 is probably not physically linked to the nebula (Brandner et al. 2000). The ProPlyD-like structures in NGC 3603 are about two orders of magnitude fainter than typical UCHRs, but have a typical extent of 9000 AU with tails extending to 21000 AU, much larger in size than the ProPlyDs in Orion.

Recent 3.4 cm radio continuum and recombination line measurements of NGC 3603 by De Pree et al. (1999), which were focussed on abundance measurements and the bright continuum emission from the ionized gas in this region, have an angular resolution of $\sim 7''$ and a 5σ sensitivity of 55 mJy. By obtaining high sensitivity and high angular resolution ($\sim 1''$–$2''$) *ATCA* observations we primarily aimed to study the radio emission of the winds from many of the early-type stars in the cluster, as well as to detect and resolve the ProPlyD-like objects and other gaseous regions in the cluster periphery. This paper will focus on the ProPlyD-like sources[7] only, which have been detected and are shown to be clearly resolved with the *ATCA*. A subsequent paper containing a detailed study of the whole NGC 3603 region based on our *ATCA* observations will follow.

2. Observations and Data Reduction

Radio continuum observations of NGC 3603 were made with the Australia Telecope Compact Array (*ATCA*) in the 6A, B, C and D configurations in five observing runs in February, April, June, September and November 2000 with a total of 60 hours assigned observing time. The observing frequencies were 4.8 GHz (6 cm) and 8.64 GHz (3 cm) with a bandwidth in each case of 128 MHz. Detailed observing parameters are given in Table 1. The three data sets were combined, reduced and analysed in MIRIAD using standard procedures. The full Stokes parameters were measured. The flux density scale was calibrated using observations of the primary calibrator, 1934–638, assuming flux densities of 2.84 and 5.83 Jy at 3 and 6 cm, respectively.

A primary beam correction was carried out. To obtain high angular resolution and filter

[7]Throughout this paper we use the term "ProPlyD-like" for these cometary-shaped objects in NGC 3603, since the identification of these objects as true ProPlyDs is premature, owing to the lack of a clear detection of a central disk or star.

the extended emission to emphasize the small scale structure we used uniform weighting of the *uv* data while omitting the shortest baselines, up to 25 kλ, respectively. We find that for a 25 kλ cutoff all bright extended nebula emission is removed from the ProPlyD-like objects even at 6 cm. Fig. 1 shows an example of a combined 3 cm radio map where a *uv* cut of 10 kλ was chosen. A zoom on the three ProPlyD-like objects is shown in Fig. 2. For the 6 cm maps a *uv* cut of 25 kλ was used. The average r.m.s. in these combined radio maps was approximately 0.2 mJy at 3 cm and 0.4 mJy at 6 cm, but varies throughout the map. The r.m.s. levels near the ProPlyD-like objects, which lie in rather empty regions, were $\sim$ 0.1 mJy at 3 cm and $\sim$ 0.2 mJy at 6 cm. The dynamic range in the 3 and 6 cm images is about 1:100. Fitting a 2D-Gaussian to the dirty beam gives FWHM values of $0\farcs94 \times 0\farcs77$ to $1\farcs06 \times 0\farcs87$ at 3 cm and $1\farcs53 \times 1\farcs23$ to $1\farcs83 \times 1\farcs49$ at 6 cm depending on the *uv* cut employed. In Fig. 2 we have restored the cleaned maps with a circular Gaussian beam of width $1''$ at 3 cm and $2''$ at 6 cm.

To create spectral index maps between 3 and 6 cm we convolved the 3 cm map with a Gaussian appropriate to achieve the resolution of the beam FWHM at 6 cm. The spectral index maps were then derived from the 6 cm and convolved 3 cm maps using a clip value of 1.0 mJy beam^{-1}, corresponding to approximately 10σ at 3 cm and 5σ at 6 cm (statistical errors). Error maps for the spectral index maps were calculated using error propagation.— We note, however, that spectral indices of extended sources as obtained from interferometric data have to be regarded with caution.

3. Results

The three ProPlyD-like sources found with the *ATCA* at 3 and 6 cm are clearly resolved, showing a head-tail extent of $\sim 4''$ (see Fig. 2). P3 shows the most pronounced head-tail structure with a 3 cm flux density ratio between head and tail of about 10:1. The tail is very well defined and at least $2''$ long, pointing away from the central star cluster. Unfortunately, P3 is rather faint in the low-sensitivity HST broad band image shown by Brandner et al. (2000); it is located outside the region of their high-sensitivity Hα image.

3.1. ProPlyD structure and fluxes

The three ProPlyD-like objects have a cometary or head-tail shape[8] at cm-radio wavelengths, matching their appearance in optical images (see Fig. 2).

Integrated radio flux densities and peak fluxes are derived by summing over the whole ProPlyD-like objects, and by fitting circular Gaussians to each object. Statistical flux uncertainties are estimated as map r.m.s. times number of beamsizes covered by the source. Dependent on the method of flux determination, beam size and *uv* cut employed to the maps (5, 10, 15, 20, 25 kλ) the resulting flux densities vary. The standard deviation of this variation is considered as systematic uncertainty. We found that the systematic uncertainties are always larger than the statistical error. In Table 2 we report the average fluxes and their uncertainties of all 3 nebulae, together with their average spectral indices derived from the integrated fluxes.

Circular Gaussians[9] are used to at least attempt disentangling the head and tail structures in these cometary-shaped objects. The radio heads of the ProPlyD-like objects are typically $2''$–$3''$ in diameter while the total head-tail extent is $\sim 4''$. P3 shows the most pronounced head-tail structure of the three (most likely due to the viewing angle) and the smallest head (diameter $\sim 2''$) among all three ProPlyD-like objects, with the largest peak flux at 3 cm while the integrated head flux is comparable. Its head-to-tail flux ratio is about 10:1, whereas in the other two ProPlyD-like objects part of the tail may be confused with the head flux density.

Both, P1 and P2, appear inclined with respect to the plane of the sky, with P1 inclined at a larger angle than P2. This can be seen in Fig. 2 where we have indicated the projected direction to the ionizing source. Fig. 3 shows the residual radio continuum image of P1 after removing a single circular Gaussian component. The residual map of P1 shows two excess emission sites, one corresponding to the tail, and a second one north of it. Recent Hα images indicate that P1 is composed of two separate cometary-shaped objects (Brandner et al. 2000). We interpret the northern excess as the second head. A two component Gaussian fit to P1 at 3 cm gives peak fluxes of 4.6 mJy beam^{-1} and 1.4 mJy beam^{-1}, and integrated flux densities of 9.9 mJy and 5.7 mJy for the two heads, with a separation of the two peaks of $1\overset{''}{.}3$. A two component model could not be applied to the lower resolution 6-cm data.

The tails of all three ProPlyD-like objects are directed away from the star cluster,

[8]The silhouette of ProPlyDs has variously been referred to as cometary, tadpole, tear-drop or simply head-tail shaped.

[9]We find that elliptical Gaussians instead of circular ones would fit too much tail flux to the head.

approximately coincident with the tails in Hα within the positional uncertainty of the radio/optical pointings (see Fig. 2; note the shift of $0\farcs5$ in declination and right ascension of the HST-image which we have employed in these figures). The uncertainty of the radio position is $\sim0\farcs15$ while HST has a pointing uncertainty of $< 1''$.

The present data were obtained in all four Stokes parameters. No polarization signal above 3σ was detected.

Possible flux variability on timescales $\gtrsim$ days expected from e.g. flaring pre-main sequence (PMS) stars with non-thermal radio spectra, cannot be tested with the present data.

3.2. Spectral indices of the ProPlyDs

The radio continuum fluxes (see Table 2) are a factor of 9 to 21 larger than those predicted by Brandner et al. (2000) assuming optically-thin thermal bremsstrahlung as the radio emission mechanism (McCullough et al. 1995), which scales with the (extinction corrected) Hα flux. The neutral part of the envelope of the ProPlyD-like object may attenuate Hα photons from the far side of the object depending on the viewing angle. However, McCullough et al. (1995) have estimated this effect to be less than 25% of the total Hα light for an isotropic ensemble of ProPlyDs. Furthermore, the reasonable coincidence of the sizes of the ProPlyD-like objects in the radio and optical band suggests that this effect is not important here. For P1 and P3 the integrated fluxes at 6 cm are higher than that at 3 cm, whereas similar flux densities were predicted. The average spectral index of each object, shown in Table 2, is calculated on the basis of the integral fluxes at 3 cm and 6 cm in this table. Modeling the uv distribution of the 6 cm map to match the uv distribution at 3 cm gives similar results.

The average spectral indices of P1 and P3 are negative (P3 only marginally), between $\alpha = -0.5 \pm 0.2$ and -0.3 ± 0.2 ($S_\nu \propto \nu^\alpha$), indicating non-thermal emission, while the spectrum of P2 ($\alpha \approx -0.1 \pm 0.2$) is in agreement with the expectation from optically thin thermal bremsstrahlung.

Hydrodynamic simulations predict spectral indices of $\alpha \approx 0$ near the ionization fronts, which can increase up to $\alpha \approx 0.6$ when considering in addition a hydrodynamically collimated jet (S. Richling, private communication). Negative spectral indices cannot be explained by this model.

Because of the high resolution and sensitivity in the radio maps, we were able to generate spectral index maps for all three ProPlyD-like objects. Fig. 4 shows examples of the spectral index maps. Here we used the radio maps shown in Fig. 2 and constrain ourselves to brightness densities greater than 1.0 mJy beam^{-1}, which corresponds to roughly 5 σ at 6 cm and 10 σ at 3 cm (based on statistical error estimates). The radio emission zone within each ProPlyD-like object appears to be inhomogeneous. The spectra in at least two of the sources appear steeper in the tail than in the head, with a tendency of positive spectral indices located towards the region facing the ionizing star cluster.

3.3. Extinction towards the ProPlyDs

Melnick et al. (1989) have derived the reddening towards NGC 3603 from UBV photometry, and found $A_V \approx 4 - 5$ mag for the cluster core. However, as can be seen in their data, the visual extinction is not uniform across the whole star forming region, but increases significantly with distance from the star cluster, mainly towards the North and the South. This is confirmed by recent VLT/ISAAC data on the basis of 4750 stars, showing that the extinction can be as high as $\mathrm{A_V} \approx 14$ mag (Brandner, private communication). For example, star MTT 68, close to P3, has $\mathrm{A_V} \approx 6.2$ mag, whereas star MTT 81 near P1 has $\mathrm{A_V} \approx 4.7$ mag, and star MTT 79 close to P2 has extinction $\mathrm{A_V} \approx 5.2$ mag. Here we use $R = A_{\mathrm{V}}/E_{\mathrm{B-V}} \approx 3.2$ as used by Melnick et al. (1989) for NGC 3603. Thus, it appears likely that P2 and P3 suffer from stronger foreground extinction than the stars in the cluster center which have on average $\mathrm{A_V} \lesssim 4.5$ mag.

Using the ratio between radio flux density and Hα flux as given by McCullough et al., (1995; their equation 5) and assuming that the radio flux density at 3 cm is dominated by thermal bremsstrahlung, we predict the Hα flux using our 3 cm radio continuum data. The predicted fluxes are then compared to the Hα fluxes measured by Brandner et al. (2000) and used to derive lower limits for the extinction, $A_{\mathrm{H}\alpha}$. (If (gyro-)synchrotron radiation dominates the radio emission, which comes from an emitting region as specified in Sect. 4.4, the derived extinction $A_{\mathrm{H}\alpha}$ would be higher, with the exact value depending on the magnetic field.) Table 3 shows the calculated fluxes (assuming $T_{\mathrm{e}} = 10^4$ K) and extinctions. Note the uncertainty in comparing different areas for which the Hα fluxes and the radio continuum fluxes have been obtained. Brandner et al. (2000) give the Hα surface brightness of the ProPlyD-like object heads, measured for a $0\farcs5$ aperture radius, whereas we quote peak fluxes per beam where the beam size is $\sim 1\farcs0 \times 1\farcs0$. For $A_{\mathrm{H}\alpha} \approx 0.85 A_{\mathrm{V}}$, we find $\mathrm{A_V} \approx 6.0$ for P1 and $\mathrm{A_V} \approx 6.7$ for P2. We find thus significant excess extinction for both ProPlyD-like objects, which may be intrinsic to the ProPlyD-like objects themselves, otherwise the extinction estimate derived from the stars is underestimated.

3.4. ProPlyD densities and mass-loss rates

Estimates for the electron/ion density inside the heads can be obtained from our radio data if thermal bremsstrahlung dominates the radio emission. This is likely to be the case for P2 and maybe P3, while for P1 the derived values should be considered as upper limits. The bremsstrahlung intensity in the radio domain for a thermal, ionized H-gas of constant density in a sphere is (Mezger and Henderson 1967)

$$S_{\rm radio} \approx 1.9 D_{\rm kpc} f_{\rm th} \theta_{\rm sec}^3 N_{e,4} N_{\rm ion,4} \nu_{\rm GHz}^{-0.1} T_4^{-0.35} {\rm mJy},$$

where $D_{\rm kpc}$ is the source distance in kpc, $\theta_{\rm sec}$ is the apparent radius of the source in arcsec, $N_{e,4}$ and $N_{\rm ion,4}$ are the densities of the thermal electrons and ions, respectively, in 10^4 cm^{-3}, $\nu_{\rm GHz}$ is the observing frequency in GHz and T_4 is the electron temperature of the ionized gas in 10^4 K. $f_{\rm th}$ is the ratio of thermally emitting to total volume of the source, and is introduced to account for the possibility of smaller emitting volumes than the apparent extent of the source. This is likely because only the outermost layers in ProPlyDs are believed to be ionized. We estimate the ProPlyD heads $\sim$ 2-3$''$ in diameter. For $T_4 = 1$ and $N_e \approx N_{\rm ion}$ we estimate the electron density by comparing the expected radio flux with the observed 3 cm ProPlyD head flux densities, and find N_e =(9, 7 and 13)$\cdot 10^3 f_{\rm th}^{-1/2}$ cm^{-3} for P1, P2 and P3, respectively. (The corresponding emission measures are EM = 5.9, 3.5 and 9.3 $\times 10^6 f_{\rm th}^{-2/3}$ cm^{-6} pc.) If the emitting volume is smaller than the total source volume, the electron density and emission measure increase accordingly. From spectral considerations the emission must be optically thin, i.e. free-free absorption may set in at frequencies lower than 4.8 GHz. Thus values of EM cannot exceed $\sim$ several 10^7 cm^{-6} pc, in order to avoid free-free absorption at frequencies above 4.8 GHz. This constrains the size of the thermally emitting volume of the 3 ProPlyD-like objects to at least 4%, 2% and 9% of the total source volumes, and consequently puts limits on the thermal electron densities in the sources: 4.5, 4.9 and 4.3 $\cdot 10^4$ cm^{-3} for P1, P2 and P3, respectively. Note that these numbers should be considered as upper limits if the observed radio flux is dominantly of non-thermal origin. These numbers are in reasonable agreement with $N_e \geq 10^4$ cm^{-3} derived from [SII] line ratios by Brandner et al. (2000). For the Orion ProPlyDs densities of order $10^5 - 10^6$ cm^{-3} have been found (Henney and O'Dell 1999). Note that our derived numbers suffer from uncertainties due to the unknown geometrical projection angle of the ProPlyD-like objects, and hence the true source diameters.

Mass loss from the ProPlyD-like objects occurs through external heating of the envelope by the far ultraviolet (FUV) radiation field from hot stars, especially from the core of NGC 3603, and subsequent evaporation. Knowing the electron density, the mass-loss rate in a wind is given by $\dot{M} = 4\pi R^2 N_e \mu m_H v_W$, with R the system radius, m_H the ion mass and v_W the evaporation velocity. Assuming a pure hydrogen gas, $\mu = 1.3$, we find

$\dot{M}/v_{20} \approx (5-10) \times 10^{-5}$ $M_{\odot}$year^{-1} for the heads of all three ProPlyD-like objects, where v_{20} is the wind velocity in units of 20 km s^{-1}. Brandner et al. (2000) found evaporation flow velocities of order 10–25 km s^{-1}. The derived upper limits for the mass-loss rates are of the same order as estimated by Brandner et al. (2000), and about two orders of magnitude higher than the typical values for the Orion ProPlyDs.

A rough estimate of the mass reservoir of the NGC 3603 ProPlyD-like objects can then be derived by multiplying the mass loss rate with an estimated evaporation time scale of $\sim 10^5$ years (Brandner et al. 2000). This gives a mass for the ProPlyD-like objects of order 1–10 $M_{\odot}$, 10–1000 times larger than for the Orion ProPlyDs. The radius of the putative disks in these massive objects can be estimated using the evaporation model of Johnstone et al. (1997) which considers the mass reservoir in a disk-like shape. We find an approximate disk radius of 2000 AU ($\approx 0.3''$) for all three NGC 3603 ProPlyD-like objects: Brandner et al. (2000) found ∼3400 AU from hydrodynamical simulations.

4. Discussion

4.1. Comparison with the ProPlyDs in the Orion and Lagoon Nebulae

The ProPlyD-like objects in NGC 3603 are 20–30 times larger and much more spectacular than those in Orion, which were detected at 2 and 20 cm with the VLA (see McCullough et al. (1995) and references therein; Henney and O'Dell (1999)).

Orion contains numerous dense clumps, originally classified as UCHRs, but now known to be ProPlyDs. Most Orion ProPlyDs have central disks, sometimes seen only in silhouette against the background light. On recent HST-images dozens of jets powered by young stars embedded in ProPlyDs have been found (Bally et al. 2000). All Orion ProPlyDs detected at radio wavelengths are non-variable thermal emitters with spectral indices between –0.1 and 0.2 (Felli et al. 1993), and located within 0.04 pc of the dominant ionizing O-star (θ^1 Ori C). The non-thermal Orion radio sources show strong variability, and are mostly associated with visible pre-main sequence (PMS) stars. Their non-thermal spectra are usually explained as due to stellar flaring activity.

G5.97–1.17 ($D = 1.8$ kpc) was originally classified as an ultracompact H II region, but is now thought to be a ProPlyD at ~ 5000 AU projected distance from the O7 star Herschel 36 in the center of M8, the Lagoon Nebula (Stecklum et al. 1998). ESO near-infrared, HST optical and VLA radio continuum observations indicate that G5.97–1.17 is a young star surrounded by a circumstellar disk that is likely being photo-evaporated by Her 36, similar to the ProPlyDs in Orion. The previous hypothesis suggested that G5.97–1.17 is a UCHR intrinsically ionized by an embedded B0 star. However, Stecklum et al. (1998) showed that G5.97–1.17 is predominantly externally ionized, and thus the spectral type of the embedded star should be later than B5. The Hα flux over $0\farcs6$ is consistent with the $\lambda = 2$ cm appearance. Optical and near infrared (NIR) continuum images show the central star is displaced from the peak of the bow shock by $0\farcs125$. NIR photometry of G5.97–1.17 revealed that its central star is extremely red, which cannot be explained by extinction laws that use spherical matter distributions. This supports the idea of the circumstellar matter surrounding the central star of G5.97–1.17 being arranged as a disk. The cm-radio spectrum of G5.97–1.17 appears flat, which is interpreted as optically thin free-free emission (Wood and Churchwell 1989; Doherty et al. 1994). No OH or H_2O masers, which are often associated with UCHRs, are known in G5.97–1.17.

In comparison, the NGC 3603 ProPlyD-like objects appear rather peculiar and spectacular. Not only are they the largest and most massive ones found so far. Exposed to an extremely strong FUV radiation field, they also suffer the largest mass losses, though their distances from the ionizing source are larger than for the Orion or Lagoon Nebula ProPlyDs. No embedded source nor disk has been found for any of the NGC 3603 ProPlyD-like objects. At cm-wavelengths they are so far the only ProPlyD-like objects showing non-thermal radio emission.

The spatial distribution of the NGC 3603 ProPlyD-like objects is also peculiar. They are not only distributed apparently along a straight line (see Sect. 4.3 for further discussion), but all three also lie clearly to the north of the ionized gas region and avoid the region north-east and south-west from the stellar cluster. This is in contrast to the Orion ProPlyDs which do not appear to be located in preferred regions of the nebula (e.g. Bally et al. (2000)). Since sequential star formation proceeding from north to south seems evident in NGC 3603 (e.g. De Pree et al. (1999)), this suggests that the ProPlyD-like structures in this region might have emerged just recently.

4.2. External versus internal ionization

A possible way to prove that the ProPlyD-like objects have indeed been ionized *externally* by the star cluster is to show that the observed radio fluxes for the ProPlyD-like objects are consistent with the number of ionizing photons they receive from the cluster stars. For simplicity we assume thermal radio emission, and note that this leads to an upper limit for the number of ionizing photons needed to produce the observed radio flux density. In this case the brightness temperature is directly proportional to the number of ionizing photons. Because NGC 3603 contains a large number of stars that are extremely hot and luminous they provide an ionizing flux that is several orders of magnitude larger than that in Orion or M 8 (see Table 4). The expected brightness temperatures at the projected distances of 1.3 pc, 2.2 pc and 2.0 pc of the ProPlyD-like objects from the ionizing source due to a Lyman flux of 10^{51}photons s^{-1} (Brandner et al. 2000) are 200 K, 70 K and 90 K at 3 cm assuming $T_4 = 1$. This is only slightly higher than our estimates derived from the *ATCA* 3 cm maps of 40 K, 30 K and 70 K for the three ProPlyD-like objects, respectively. We can also compare the number of ionizing photons required to deliver the observed flux densities at the location of the ProPlyD-like objects, and compare this number with the number of Lyman photons they receive from the star cluster. Noting that the ProPlyD-like objects subtend a fraction of (6, 3 and 2)$\cdot 10^{-5}$, of the total solid angle seen by the cluster stars, they thus receive (6, 3 and 2)$\cdot 10^{46}$ photons s^{-1}, respectively. On the other hand, the required number of ionizing photons at the location of each ProPlyD-like object to deliver the observed radio flux density is about $2 \cdot 10^{46}$ photons s^{-1} in all three cases. These comparisons show that the number of required Lyman photons is slightly lower than provided by the star cluster, and thus would even allow an additional dust attenuation and/or, more likely, longer linear distances between the ProPlyD-like objects and the ionizing source in the external ionizing scenario. Significant ionizing power from within the ProPlyD-like objects appears therefore unlikely, which puts the spectral type of any central stars to later than $\sim$B1, and hence mass to below ~ 10 M$_\odot$.

4.3. Do the ProPlyD-like objects host disks ?

The present radio data as well as the recently published HST/VLT-images do not provide any direct evidence that the observed ProPlyD-like objects in NGC 3603 host any (proto-)stellar objects or disks. To a limiting K_s-magnitude of 18, no circumstellar disk or central stellar object in any of the three ProPlyD-like objects has been detected by HST+VLT observations. Instead the cometary-shaped nebulae may rather be massive emission regions photo-ionized by the radiation from the star cluster. Mellema et al. (1998) have presented model calculations for such clumps, called FLIERs or ANSEA which are commonly located along the major axis towards the ionizing source. Indeed, all three ProPlyD-like objects apparently lie approximately along one straight line, with the outflow source, Sher 25, located roughly midway between P1 and P3. Although the bipolar outflow from Sher 25 appears not to point in the direction of any of the three ProPlyD-like sources, the ring-like structure around Sher 25, roughly perpendicular to its jet, has been shown to expand with a velocity of ~ 30 km s^{-1} (Brandner et al. 1997), and could in principle be related to the origin of the ProPlyD-like clumps. In addition, models such as the FLIER model which are not based on disk-like mass distributions typically give short evaporation times, inconsistent with the distance of the ProPlyD-like objects from Sher 25 (W. Brandner, private communication) and the approximate date of the mass-loss event about 6630 years ago in Sher 25 (Brandner et al. 1997). Thus, the existence of such features at large distances from the cluster centre appears to favor models where most of the material is concentrated in compact structures such as disks. The actual presence of disk-like structures is however not confirmed.

4.4. The possible origin of the non-thermal emission

The significantly non-thermal spectrum ($\alpha \ll 0, S_\nu \propto \nu^\alpha$) from at least one of the three NGC 3603 ProPlyD-like objects (P1; P3 seems to be marginally non-thermal) appears to be steepest ($\alpha < -0.5$) in the tail, slightly flatter ($\alpha = -0.5$ to 0.1) in the head, and have a tendency of positive spectral indices ($\alpha > 0$) located towards the region facing the ionizing star cluster rather than away from it. This is not expected from non-thermal radio emission from a wind–wind collision region. The non-thermal radiation must originate rather from inside the ProPlyD-like objects, either from their putative central stars hidden behind thick material, the surrounding disks or the envelopes. A stellar origin analogous to active star coronal emission seems to be unlikely because of the extended nature of the observed source. Non-thermal radio spectra could be produced by a population of energetic particles emitting synchrotron, gyrosynchrotron or gyroresonance radiation in a magnetic field. For gyrosynchrotron radiation the emission is concentrated at harmonic numbers $s = \nu/\nu_B = 10-100$ (where $\nu_B \approx 2.8{\cdot}10^{-3} B_G$ GHz is the gyrofrequency, B_G is the magnetic field strength in Gauss), and thus magnetic fields strengths of order $B \approx 20 - 200$ G are required. These high field values cannot be present in extended sources, which leaves synchrotron radiation as the only plausible emission mechanism.

Disk or envelope, whatever the ultimate source might be, the negative spectral indices suggest optically thin non-thermal processes as the dominant radiation mechanism in P1, and maybe P3. One could argue that the shock created by the evaporation flow predicted in ProPlyD models could accelerate charged particles within the objects. Other possibilities may be inflow-outflow activity causing shocks during the early stage of star formation, compression and reconnection of magnetic fields in the collapsing envelope, or magnetic reconnection in star–disk interactions in Young Stellar Objects leading to production of energetic particles. Magnetic fields are known to exist in Molecular Clouds (Crutcher 1999), and therefore it appears plausible that gas clumps still contain “fossil” fields. In a magnetized plasma, acceleration due to particle collisions and subsequent bremsstrahlung can often be negligible in comparison with acceleration due to gyration around the field lines. In place of free-free emission, there is then synchrotron emission from energetic particles. The negative radio spectral indices in P1 and P3 are conveniently explained by non-thermal particle spectra. Because thermal bremsstrahlung is proportional to $N_e^2 T_e^{-1/2}$ and synchrotron emission is proportional to $N_e B^\beta$ ($\beta > 0$), the former dominates if the density is high enough, or if the temperature or field strength is low enough. Indeed the electron densities found in the NGC 3603 ProPlyD-like objects are ∼two orders of magnitude smaller than in the Orion ProPlyDs (see Table 4). The different energy dependencies of the two kinds of emission may lead to one dominating at low frequencies and the other at high frequencies.

A lower limit for a possible magnetic field is given by the Razin-Tsytovich effect. In order to avoid a Razin-suppression of the radio spectrum above $\lambda = 6$ cm the magnetic field cannot be smaller than $\sim 10^{-5}$ G for an electron density of 10^4 cm^{-3} in the emission region. On the other hand, to avoid gyroresonance absorption above $\lambda = 6$ cm the field strength cannot be higher than 10^3 G. The equipartition magnetic field, the minimum possible value in flare loops, for a $T_e = 10^4$ K particle distribution with density 10^4 cm^{-3}, is $\sim 10^{-3}$ G. Note that synchrotron photons of energy 4.8 GHz in a 10^{-5} G field must have been produced by ~ 10 GeV electrons. Efficient particle acceleration may occur, e.g., at the ProPlyD surface, from flow amplification of even very weak ambient magnetic fields followed by local reconnection events (e.g. Shore & Larosa (1999)).

The flux density from a homogeneous sphere with diameter l due to synchrotron radiation in a uniform field and a low energy cutoff $E_{\rm min,MeV}$ in units MeV of a $E^{-\alpha_e}$ particle distribution with $\alpha_e = 2$ spectral index[10] is given by (e.g. Dulk 1985)

$$S_{\nu,\rm syn} \approx 5 \times 10^{18} N_{e,nt,4} B_G^{1.5} E_{\rm min,MeV} l_{\rm pc}^3 D_{\rm kpc}^{-2} \nu_{GHz}^{-0.5} \ {\rm mJy}\,.$$

The non-thermal electrons might have been energized by e.g. shock acceleration or magnetic reconnection events, out of the pool of thermal particles, or they may be Galactic cosmic rays penetrating the starforming region. In the latter case $N_{e,nt} \approx 10^{-2} \ldots 10^{-1}{\rm cm}^{-3}$ and $\alpha_e \approx 2.4$, and thus $B \approx 10^{-3}$ G (for $E_{\rm min,MeV} = 1$). For the former case, because energy is conserved, the production efficiency of the high energy particles is related to the properties of the thermal background particles, and vice versa. Realistic non-linear diffusive particle acceleration scenarios typically yield $N_{\rm e,nt}/N_{\rm e} \sim 10^{-5} - 10^{-1}$ (i.e. the fraction of total electrons which end up with high energies; e.g. Ellison et al. (2000)), while magnetic reconnection might be as efficient as $N_{\rm e,nt}/N_{\rm e} \sim 0.01$ for the present densities and temperature (Tandberg-Hanssen & Emslie 1988). Since the thermal electron density N_e cannot be significantly smaller than $\approx 10^4{\rm cm}^{-3}$ (derived from [SII] line ratios; see Sect.3.4), and $N_{\rm e,nt} \leq N_e$ if thermal and non-thermal electrons have the same source, we find that the size

[10]Shock acceleration typically predicts a E^{-2} power law, which we use as a reasonable assumption here.

of the actual magnetized volume emitting non-thermal radiation must be smaller than the appearance of the ProPlyD-like object on the sky for this case. If particle trapping is at work, $N_{\mathrm{e,nt}} \geq N_{\mathrm{e}}$ is possible, and consequently the ratio of emitting to total volume of the ProPlyD-like object becomes even smaller.

The present data, however, do not allow to quantitatively constrain the actual size of the source responsible for the non-thermal radiation.

We note that the recent discovery of variable X-ray emission from some ProPlyDs in Orion by Schulz et al. (2000) support the idea of a non-thermal emission volume smaller than the appearance of the ProPlyD-like object on the sky. The size of the emitting region was estimated on the basis of variability arguments to order 1–10 AU.

5. Summary and Conclusions

The three massive ($\sim$1–10 $\mathrm{M}_\odot$) ProPlyD-like nebulae in NGC 3603, which have recently been discovered by Brandner et al. (2000), have been clearly detected and resolved with the *ATCA* at 3 and 6 cm, with one of them likely to be composed of two cometary-shaped objects. Their flux densities are about 10–20 times higher than expected from the Hα measurements, and a non-thermal average spectrum can be associated with at least one of the three ProPlyD-like sources. This is the first time that non-thermal radio emission has been detected from ProPlyD-like sources. Our spectral index maps show that the emission region is rather inhomogeneous, with negative spectral indices in the tail and part of the head whereas positive spectral indices, indicating thermal free-free emission, tend to be detected from a small region facing the star cluster.

We derive upper limits for the mass-loss rates of 10^{-5} $\mathrm{M}_\odot\,\mathrm{year}^{-1}$ and electron densities of 10^4 cm^{-3}. These are in reasonable agreement with estimates from recent HST-images.

We show that synchrotron emission from a magnetized, relativistic, non-thermal particle population may explain the non-thermal spectral regions. Energetic electrons necessary for synchrotron radiation may be produced through shocks or by magnetic reconnection out of the pool of thermal particles, or may be Galactic cosmic rays.

A stellar origin of the observed flux densities appears unlikely considering that the sources are extended. Thus magnetic fields, which have been neglected in ProPlyD models so far, are possibly associated with the ProPlyD envelopes or disks, and appear to be crucial in understanding the physical processes in these ProPlyD-like objects.

Melnick et al. (1989) have shown that an inhomogeneous dust distribution in NGC 3603 causes increasing extinction with distance from the star cluster. In particular, the extinction at the location of the ProPlyD-like objects is estimated to lie between $A_V \approx 5-6$ mag. Extinction estimates derived from the radio- to Hα-luminosity ratio are 1–2 magnitudes higher.

The ultimate discovery of the so-far undetected disks, which are thought to be part of all ProPlyDs, would give important hints about the origin of the extremely high and non-thermal radio fluxes and the nature of the cometary-shaped clumps seen in NGC 3603. This may be accomplished in future mm observations with an upgraded *ATCA*.

We are grateful to Wolfgang Brandner for providing the HST image of NGC 3603 to overlay on our radio images, for interesting discussions and carefully reading the manuscript. We thank Jessica Chapman, Jim Caswell, Simon Johnston, Tylor Bourke and Sergey Marchenko for reading the manuscript and many constructive comments which improved our paper significantly. AM acknowledges a postdoctoral bursary from the Quebec Government. AFJM thanks NSERC (Canada) and FCAR (Quebec) for financial support. IRS acknowledges the receipt of a PPARC Advanced Fellowship.

REFERENCES

Bally, J., O'Dell, C.R. and McCaughrean, M.J. 2000, AJ, 119,2919

Brandner, W., Chu, Y.-H., Eisenhauer, F., Grebel, E.K., Points, S.D. 1997, ApJ, 489, L153

Brandner, W., et al. 2000, AJ, 119, 292

Churchwell, E. 1990, A&A Rev., 2, 79

Crowther, P.A. and Dessart, L. 1998, MNRAS, 296, 622

Crutcher, D., 1999 ApJ, 520, 706

De Koter, A., Heap, S.R. and Hubeny, I. 1997, ApJ, 477, 792

De Pree, C.G., Nysewander, M.C. and Goss, W.M. 1999, AJ, 117, 2902

Doherty, R.M., Puxley, P., Doyon, R. and Brand, P.W.J.L. 1994, MNRAS, 266, 497

Dulk, G.A. 1985, ARA&A, 23, 169

Ellison, D.C., Berezhko, E.G. & Baring, M.G., ApJ, 540, 292

Felli, M., Taylor, G.B., Catarzi, M., Churchwell, E. and Kurtz, S. 1993, A&AS, 101, 127

Henney, W.J. and O'Dell, C.R. 1999, AJ, 118, 2350

Johnstone, D., Hollenbach, D., Störzer, H., Bally, J., Devine, D. and Southerland, R. 1997, BAAS, 189, No. 49, 12.

McCullough, P.R. et al. 1995, ApJ, 438, 394

Mellema, G., Raga, A.C., Canto, J., Lundquist, P., Balick, B., Steffen, W. and Noriega-Crespo, A. 1998, A&A, 331, 335

Melnick, J., Tapia, M. and Terlevich, R. 1989, A&A, 213, 89

Mezger, P.G. and Henderson, A.P. 1967, ApJ, 147, 471

Moffat, A.F.J., Drissen, L., and Shara, M. 1994, ApJ, 436, 183

O'Dell, C.R., Wen, Z. & Hu, X. 1993, ApJ, 410, 6960

Schulz, N.S., Canizares, C., Huenemoerder, D., Kastner, J.H., Taylor, S.C. and Bergstrom, E.J. 2000, ApJ, in press

Shore, S.N. & Larosa, T.N. 1999, ApJ, 521, 587.

Stapelfeldt, K., Sahai, R., Werner, M., & Trauger, J. 1997, in ASP Conf. Ser. 199, Planets Beyond the Solar System and the Next Generation of Space Missions, ed. D. Soderblom (San Francisco:ASP), 131

Stecklum, B., Henning, T., Feldt, M., Hayward, T.L., Hoare, M.G., Hofner, P and Richter, S. 1998, AJ, 115, 767

Tandberg-Hanssen, E. & Emslie, A.G., 1988, in: The Physics of Solar Flares, Cambridge

Wood, D.O.S. and Churchwell, E. 1989, ApJS, 69, 831

This preprint was prepared with the AAS LaTeX macros v5.0.

Fig. 1.— 3-cm continuum map with a *uv* cutoff at 10 kλ of NGC 3603 overlaid onto the Hα and broad band HST-image from Brandner et al. (2000). Note that in this radio map the small scale structure is emphasized due to our chosen *uv*-cutoff in the data analysis. For smoothing purposes the map was restored with a $2'' \times 2''$beam size. The brightest, extended continuum regions correspond to the heads of the giant gaseous pillars, showing evidence for the interaction of ionizing radiation with cold molecular hydrogen clouds. The radio emission from IRS 9, a deeply enshrouded association of protostars at the foot of the South-Eastern pillar, will be discussed in a forthcoming paper (Mücke et al., in prep.). The three nebulae indicated are the ProPlyD-like sources; their tadpole shape is shown in Fig. 2. The contour levels at 3 cm are -0.8, 0.8, 2.0, 4.0, 6.0, 12.0, 24 and 48 mJy beam^{-1}. The beam is shown inside the box at the bottom left corner. North is to the top and East to the left.

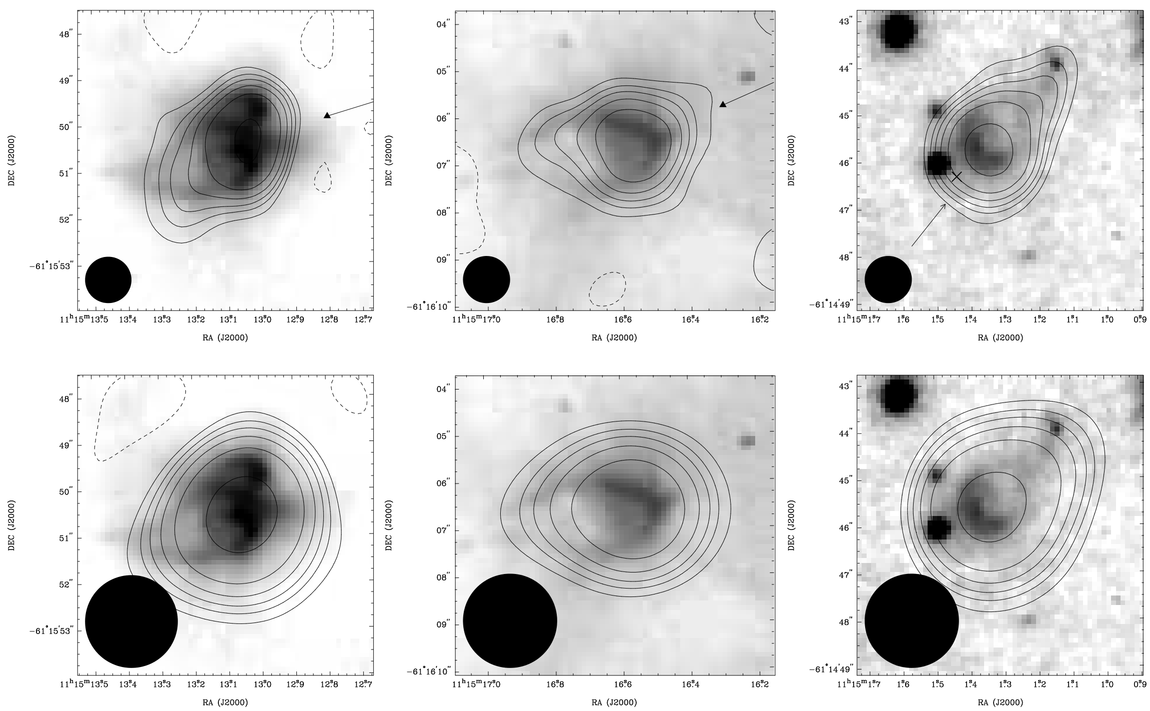

Fig. 2.— *ATCA* 3 cm (upper row; *uv* cutoff at 10 kλ) and 6-cm (lower row; *uv* cutoff at 25 kλ) radio continuum contour maps of the three ProPlyD-like sources, numbers 1–3 from left to right, overlaid onto the Hα image from Brandner et al. (2000) for P1 and P2, and onto the HST broad band image for P3. The contour levels for the 3 cm maps are -0.45, 0.45, 0.75, 1.05, 1.5, 2.25 and 4.5 mJy beam^{-1}, and for the 6 cm maps are -0.9, 0.9, 1.5, 2.1, 3.0, 4.5 and 9.0 mJy beam^{-1}. The beam is shown in the bottom left corner of each map. The Hα images have been shifted $0\farcs5$ to the North and $0\farcs5$ to the East in better alignment with the radio images. The arrows indicate the directions projected onto the sky from which the stellar cluster winds come. The cross near P3 indicates the position of the *Chandra* X-ray source.

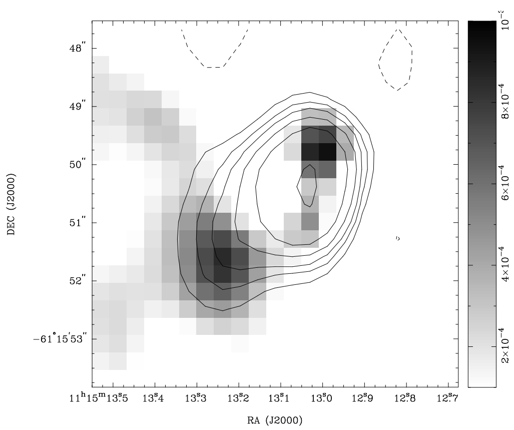

Fig. 3.— *ATCA* 3 cm residual image of P1 after subtracting a single circular Gaussian overlaid onto its unsubtracted brightness contour map as shown in Fig. 2a. The contour levels correspond to -0.3, 0.3, 0.5, 0.7, 1.0, 2.0 and 5.0 mJy beam^{-1}. P1 appears to possess two heads.

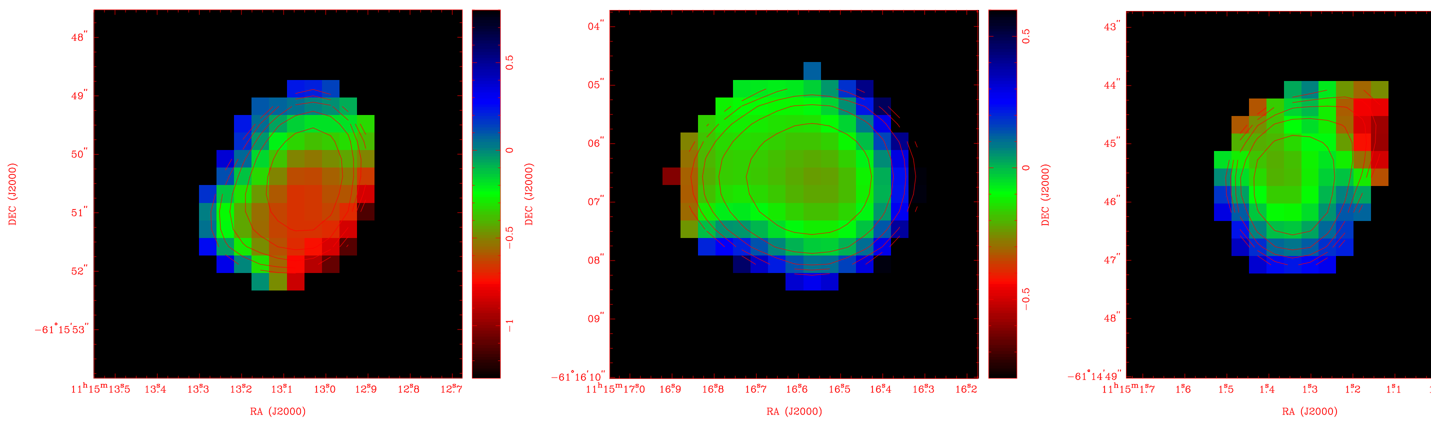

Fig. 4.— Examples of radio spectral index maps (α; colour-coded) with the corresponding uncertainty levels ($\Delta\alpha$; contours) for P1, P2 and P3 (from left to right) derived from the radio maps shown in Fig. 2. The contour levels are $\Delta\alpha$ = 0.2, 0.3, 0.4, 0.5 and 0.6. The 3 and 6 cm flux densities used to produce these maps have been clipped at 1.0 mJy beam^{-1}. Note the large spectral index uncertainties at the rim of the ProPlyD-like objects due to the low flux densities there.

Table 1: Observing parameters.

Date (local time)	February 9/10	April 8/9	June 19	Sept. 13/14	Nov. 8/9
Configurations	6A	6D	6B	6A	6C
Time on source	561 min.	514 min.	480 min.	513 min.	543 min.
Pointing position					
RA (J2000)	$11^{\rm h}\,15^{\rm m}\,07^{\rm s}$				
DEC (J2000)	$-61^\circ\,16'\,00''$				
Total bandwidth	128 MHz				
No. of channels	32				
Frequencies	8640 MHz, 4800 MHz				
Beam size	$\sim1''\times\ 1''$(3 cm)				
	$\sim2''\times\ 2''$(6 cm)				
average r.m.s. near	$\sim$0.1 (3 cm)				
ProPlyDs [mJy beam^{-1}]	$\sim$0.2 (6 cm)				
Flux calibrator	1934–63				
Phase calibrator	1059–63				

Table 2. Position, fluxes and spectral indices of the ProPlyD-like objects.

Name	P1		P2		P3	
λ	3 cm	6 cm	3 cm	6 cm	3 cm	6 cm
Radio position[1] RA,DEC (J2000)	11:15:13.042, –61:15:50.38	11:15:13.058, –61:15:50.53	11:15:16.557, –61:16:06.57	11:15:16.579, –61:16:06.62	11:15:01.336, –61:14:45.69	11:15:01.330, –61:14:45.53
Peak flux (mJy beam^{-1})	4.3 ± 0.5	11.5 ± 1.6	3.2 ± 0.4	7.8 ± 1.1	5.6 ± 0.7	10.9 ± 1.4
Integrated flux[2](mJy)	13.9 ± 1.1	18.1 ± 1.2	11.3 ± 1.4	12.1 ± 0.7	14.1 ± 1.0	16.5 ± 0.7
Spectral index of whole source[3]	-0.5 ± 0.2		-0.1 ± 0.2		-0.3 ± 0.2	
$I_{\mathrm{H}\alpha}$[4](cm^{-2} s^{-1})	0.56	0.56	0.20	0.20	···	···
Predicted radio flux[5](mJy)	1.56 ± 0.39	1.65 ± 0.41	0.56 ± 0.14	0.59 ± 0.15	···	···

Note. — The position of P3 given by Brandner et al. (2000; their Table 1) contains a typographical error.

[1]Positions correspond to the radio locations of the ProPlyD-like object heads.

[2]The quoted 3 cm and 6 cm integral fluxes are derived from images with different resolution.

[3]Flux density $S_\nu \propto \nu^\alpha$, α = spectral index.

[4]Hα flux corrected for an assumed foreground extinction in Hα of $A_{\mathrm{H}\alpha} = 4$ mag.

[5]See Brandner et al. (2000): assuming an electron temperature for the Donised gas of 10^4 K; the flux uncertainty is less than 25% due to attenuation by the neutral envelope of the ProPlyD-like object itself as estimated by McCullough et al. 1995 (see text).

Table 3: Fluxes and derived extinction

ProPlyD		1	2	3
3 cm peak flux	[mJy beam^{-1}]	4.3	3.2	5.6
predicted Hα peak flux	[cm^{-2} s^{-1}]	1.5	1.1	2.0
derived $A_{\mathrm{H}\alpha}$	[mag]	5.1	5.7	—

Table 4: Comparison with other known ProPlyDs.[1]

		Orion Nebula M 42	Lagoon Nebula M 8, NGC 6523	NGC 3603
distance	[kpc]	0.45	1.8	6.1
central star(s)		Θ^1 Ori C	Herschel 36	cluster
star type(s)		O7	O7.5V	3 WNs+ ∼70 O stars
$L_{\rm bol}$	[$L_\odot$]	$\sim 10^5$	$\sim 10^5$	2×10^7
Lyman flux	[photons s^{-1}]	$\sim 8 \cdot 10^{48}$	2×10^{48}	10^{51}
extinction	[mag]	4–6	~ 5	4–6
masers		H_2O, SiO	none known	OH, H_2O, CH_3OH
number of ProPlyDs		> 150	1 = G5.97–1.7	3
head size	[AU]	45–355	1080	7200–10800
distance to central stars	[pc]	0.01–0.15	0.024	1.3, 2.2, 2.0
radio flux	[mJy]	0.3–1.4	17	10–12
brightness temp.	[K]	$\sim 10^2 - 10^3$	~ 1500	30–90
emission measure	[pc cm^{-6}]	$8 \cdot 10^6$	$(0.3 - 2) \cdot 10^8$	$(3 - 9) \cdot 10^6 f_{\rm th}^{-2/3}$[2]
electron density	[cm^{-3}]	$10^5 - 10^6$	$(4 - 20) \cdot 10^4$	$\sim 10^4$
mass loss rate	[$M_\odot$ yr^{-1}]	$1.2 \cdot 10^{-7}$	$7 \cdot 10^{-7}$	10^{-5}
bow shock distance	[AU]	~ 100	540	44400,17400, $\cdots$
velocity	[km s^{-1}]	$\sim 10 - 15$	~ 10	10–25
evap. time scale	[years]	$\sim 10^4$	$\sim 10^5$	$\sim 10^5$
ProPlyD mass	[$M_\odot$]	0.01–0.1	~ 0.1	$\sim 1 - 10$
disk radius	[AU]	27–175	160	3400
disk mass	[$M_\odot$]	$\sim (0.5 - 20) \cdot 10^{-3}$	$\sim 6 \cdot 10^{-2}$	not known

[1] Detailed information on the NGC 2024 ProPlyD is not available.

[2] See Sect. 3.4.

References. — Stecklum et al. 1998, Brandner et al. 2000, Henney & O'Dell 1999, McCullough et al. 1995